

## Temperature effects on the vibration–rotation spectrum of a physisorbed diatomic

John E. Adams

Citation: *The Journal of Chemical Physics* **87**, 4249 (1987); doi: 10.1063/1.452882

View online: <http://dx.doi.org/10.1063/1.452882>

View Table of Contents: <http://scitation.aip.org/content/aip/journal/jcp/87/8?ver=pdfcov>

Published by the [AIP Publishing](#)

---

### Articles you may be interested in

[Semiclassical vibration–rotation spectra of gaseous and physisorbed molecules](#)

*J. Chem. Phys.* **84**, 3589 (1986); 10.1063/1.450194

[Influence of VibrationRotation Interaction on Line Intensities in VibrationRotation Bands of Diatomic Molecules](#)

*J. Chem. Phys.* **23**, 637 (1955); 10.1063/1.1742069

[The VibrationRotation Spectrum of Silyl Iodide](#)

*J. Chem. Phys.* **23**, 215 (1955); 10.1063/1.1740546

[The Vibration—Rotation Spectrum of HDO](#)

*J. Chem. Phys.* **21**, 1302 (1953); 10.1063/1.1699197

[VibrationRotation Spectrum and Structure of Monochlorosilane](#)

*J. Chem. Phys.* **19**, 138 (1951); 10.1063/1.1747975

---



# Temperature effects on the vibration-rotation spectrum of a physisorbed diatomic

John E. Adams

*Department of Chemistry, University of Missouri-Columbia, Columbia, Missouri 65211*

(Received 1 April 1987; accepted 16 July 1987)

We report the results of a study of temperature influences on the vibration-rotation line shape of a prototypical physisorption system,  $\text{HCl}/\text{Ar}$  (111). Two particular features of the problem are examined, the first being the effect of surface motion (phonons) on the line shapes deriving from several different rotational transitions within the fundamental vibrational band. On the whole, phonon contributions are found to be significant at the lowest and highest rotational energies but negligible between the two limits. The second feature of interest is the effect of changing the system temperature on the line shape arising from a single transition. Results obtained in this investigation are consistent with experimentally determined temperature dependences for other systems where dephasing is thought to represent an important line broadening mechanism.

## I. INTRODUCTION

Energy loss spectroscopies can in principle provide a wealth of information regarding both the structure and the dynamics of adsorbed species,<sup>1</sup> but at present it is not always obvious how one *quantitatively* deconvolutes the various bits of information concerning bonding, energy relaxation, and interadsorbate forces that are contained in the observed peak positions and line shapes. This problem is becoming particularly acute since not only are more spectra of this sort [especially the infrared reflection absorption spectra (IRAS) and electron energy loss spectra (EELS)] being reported, but also higher resolution is being achieved. In order to give just one important example of a system from which useful dynamical information has been extracted, we note the recent observations of discrete peaks in high-resolution EELS spectra of  $\text{H}_2$  molecules physisorbed on several different surfaces [specifically  $\text{Ag}(111)$ ,<sup>2</sup>  $\text{Cu}(100)$ ,<sup>3</sup> and the basal plane of graphite<sup>4</sup>], with the rotation and vibration-rotation excitation frequencies obtained from such measurements being found to be very near the gas-phase values. These results suggest that here the adsorbed molecules behave as if they are three-dimensional rotors, and thus any energy barriers to rotation arising due to the molecule-surface interaction must be of a magnitude less than or roughly equal to the molecule's rotation constant. But clearly a physisorption system of this type represents a particularly simple dynamical limit; in most cases one must expect a significant perturbation of the motion of the adsorbed species. It is important, therefore, that we recognize the spectral signatures of the various influences that might give rise to such a perturbation if we are to make much progress in understanding fluid-solid interfacial dynamics.

In a previous paper<sup>5</sup> (hereafter, I) we have described a straightforward means for calculating the spectral line shapes of adsorbates that is based on a semiclassical formalism developed by Marcus and co-workers.<sup>6</sup> This methodology, applied in I to a simple physisorption system, involves the use of classical trajectories in order to obtain the time dependence of the adsorbed molecule's dipole moment, from

which a line shape function is calculated via application of a Fourier transform. A classical-quantum correspondence principle gives the prescription for choosing the initial conditions for the trajectories, with initial classical action variables for vibration and rotation being taken as the arithmetic averages of the quantum numbers indexing the initial and final states of the spectral transition. (The accuracy of this procedure for selecting initial action variables strictly depends, of course, on a knowledge of the "good" quantum numbers for the states involved in the transition. However, in an adsorbate-substrate system one in general does not know these good quantum numbers, since the question of how to compute semiclassical eigenvalues for a system having many degrees of freedom remains to be answered satisfactorily, although considerable progress has been made in solving this problem in recent years.<sup>7</sup>) The resulting line shapes have suggested that at low molecular rotational energies the adsorbate dynamics is dominated by elastic rotational dephasing collisions with the surface and that the rate of dephasing increases upon the introduction of additional rotational energy (the spectral lines broaden as the initial rotational action variable is increased). Eventually the adsorbate-surface collisions become sufficiently frequent and violent that the molecule begins to tumble across the surface. Now a quite different spectrum, one characterized by very broad lines (linewidths here are tens of  $\text{cm}^{-1}$ ), is observed. At even higher rotational energies, though, the system enters another dynamical regime in which the principal motion of the molecule is on the average just a rotation in a plane parallel to the surface plane. This relatively unhindered rotation is easily identified from the spectrum, since it is associated with spectral lines that differ little from those observed for the free molecule.

There is, however, an obvious shortcoming of the work described in I, that being the neglect of surface atom motion and hence of phonon effects. (We have also omitted any possibility of coupling to electronic degrees of freedom of the solid. Although such effects are thought to play an important role in the decay of excited states of adsorbates on metal surfaces,<sup>8</sup> they can be ignored in the case of an insulator

surface such as the one considered in I and in the present work.) The study described here corrects the omission by including the full dynamics of the atoms of the surface layer, with the initial conditions for trajectories being chosen in accordance with a fixed system temperature. Again the prototypical physisorption system HCl/Ar(111) is taken as the subject of our study. First we examine the phonon effects on the spectra deriving from different vibration-rotation transitions at a single fixed temperature. We then restrict our attention to a single spectral transition (presumably the most important one) occurring at different system temperatures. Finally a comparison is made between these results obtained at various temperatures and the analogous static-surface results; the static-surface calculations, since they do include adsorbate diffusion, might still display a temperature dependence even though phonon modes are ignored.

## II. CALCULATIONS

### A. Theory

The calculation of line shapes on the basis of quasiclassical trajectories has been pioneered by Marcus and co-workers<sup>6</sup> as a means for studying intramolecular energy flow in a variety of model systems. They have shown the resulting spectral intensities generally to be in very good agreement with the analogous quantum results for a large number of vibrational transitions, corresponding not only to fundamental bands but also to combination and overtone bands. The extension of these methods to systems described by realistic molecular potentials by Stine and Noid<sup>9</sup> and the further application of the formalism by us to vibration-rotation transitions<sup>5</sup> have also met with success. (We also note that Berens and Wilson<sup>10</sup> have reported calculations of the line shapes of vibration-rotation bands, although their use of purely classical trajectory methods has led to only the envelope of the absorption lines being obtained. Such a limitation was not particularly significant for the CO-Ar solution systems that constituted their primary interest.) Since a full description of the process by which one computes the spectral line shapes has been given previously in several places,<sup>5,6</sup> we will mention here only an outline of the method and instead will concentrate on the application to our particular adsorbate-surface system.<sup>11</sup>

The fundamental equation on which the entire formalism is based is the expression for the line shape function in terms of the dipole autocorrelation function<sup>12</sup>

$$I(\omega) = (2\pi)^{-1} \int_{-\infty}^{+\infty} dt \langle \mu(0) \cdot \mu(t) \rangle e^{-i\omega t}, \quad (2.1)$$

where here  $\mu(t)$  is a Heisenberg dipole moment operator. It is easy to see how one then transforms this quantum mechanical relationship into a classical one by replacing the time-dependent operators with classical dipole moment functions. While Eq. (2.1) can be used in its present form, a more convenient approach to calculating the line shape function makes use of the alternate expression

$$I(\omega) = (2\pi)^{-1} \lim_{T \rightarrow \infty} T^{-1} \left\langle \sum_{j=x,y,z} \left| \int_0^T dt \mu_j(t) e^{-i\omega t} \right|^2 \right\rangle, \quad (2.2)$$

that, while not identical with Eq. (2.1), differs only by a term that vanishes in the long-time limit.<sup>13</sup> The computational strategy that yields  $I(\omega)$  should now be fairly obvious: generate classical trajectories, extract from them the values for the Cartesian components of the dipole moment, and carry out a Fourier transform of the resulting moments. A further expansion of the dipole moment components in real Fourier series was also incorporated into the present work, the details of such an expansion being given elsewhere,<sup>5,6(b)</sup> but we could have chosen just as easily to use Eq. (2.2) directly.

To this point, however, we have not taken into account the quantum-classical correspondence rule that relates our trajectories to specific quantum transitions. This semiclassical feature of the method arises in the selection of initial conditions for the trajectories, giving a prescription for choosing initial action variables (the corresponding initial angle variables are chosen at random from the appropriate distributions). As indicated in I, for many systems of interest the initial action variables may be taken to be the arithmetic averages of the quantum numbers associated with the initial and final states involved in the transition. Even though this choice is based on an approximation to an analytic result that is strictly valid only for a harmonic oscillator,<sup>14</sup> it has been shown to give accurate intensities in a number of anharmonic (and therefore realistic) systems as well.

### B. Model and computational method

As indicated above, we have chosen HCl physisorbed on an Ar(111) crystal face as our model system to be studied. The potentials adopted in I, a Dunham oscillator potential representing the force between the hydrogen and chlorine atoms and sums of truncated Lennard-Jones potentials of the form proposed by Weber and Stillinger<sup>15</sup> (with parameters given by Diestler<sup>16</sup>) describing the two-body interactions between hydrogen and argon and between chlorine and argon, are again employed here. Likewise, we once more make use of the Padé approximant form for the dipole moment function of HCl that has been reported by Ogilvie, Rodwell, and Tipping.<sup>17</sup> In the present work, since the surface argon atoms are permitted to move, it is necessary to include a model of the argon-argon interactions; a summation of the pairwise-additive truncated Lennard-Jones potentials of Weber and Stillinger<sup>15</sup> (which is known to reproduce the desired fcc crystal structure) also is used here.

To represent the solid surface, we make use of the template model,<sup>18</sup> in which a rectangular slab composed here of 24 atoms per layer and two atomic layers is replicated in two dimensions by the imposition of periodic boundary conditions. In the lower layer the atoms are held fixed in their equilibrium positions, providing a template that preserves the correct relative geometry of the atoms in the moving top layer. Positions for the atoms of this top layer at the beginning of a trajectory and the position of the HCl molecule relative to the surface are determined by means of a thermally biased random walk (Monte Carlo with Metropolis sampling<sup>19</sup>) of the 24 Ar atoms, H, and Cl at a particular surface temperature. The only constraints placed on the system during this randomization and equilibration procedure are that

the HCl bond length is held fixed at its equilibrium value and that the distance between the molecule and the surface is kept within the truncation range of the H-Ar and Cl-Ar potentials. Instantaneous system snapshots generated in this manner are then combined with suitably chosen velocities to yield the sets of initial conditions for the trajectories. The choice of those velocities is made in the following way. Having selected action variables for molecular vibration and rotation in accordance with the correspondence rule mentioned in Sec. II A above, we calculate total vibrational and angular momenta and apportion them between H and Cl using standard techniques.<sup>20</sup> In addition, a random sampling from the appropriate Boltzmann distribution gives the components of the molecule's center-of-mass velocity which are added to the velocity components stemming from the internal degrees of freedom. Finally, the initial velocities of the argon atoms in the uppermost solid layer are chosen at random also by sampling from a Boltzmann distribution corresponding to the chosen system temperature.

The 156 equations of motion (three coordinate and three velocity equations for each of the 24 moving Ar atoms, H, and Cl) are integrated using the so-called "velocity form" of the Verlet algorithm described by Swope *et al.*<sup>21</sup> In doing so, we have departed from our past methods in which an integration algorithm of much higher accuracy (Adams-Moulton fifth-order predictor/sixth-order corrector with a fourth-order Runge-Kutta-Gill startup) was used routinely. The most significant advantage of a Verlet-type algorithm is not that the routine is itself simpler, but rather that it requires only a single calculation of the forces per integration step, with the force calculation accounting by far for the largest fraction of the expended computational time. In a direct comparison of the spectra obtained using the high- and low-accuracy integration algorithms, we found no appreciable difference between the two results. Such an outcome actually is not surprising, since the integration errors introduced by the Verlet algorithm can be viewed as contributing white noise to the calculation of the time dependence of the dipole moments, and random noise of this sort is filtered out when the Fourier transform [Eq. (2.2)] is taken. We also should note here another feature of the computations that has been introduced in order to reduce the amount of computer time required for obtaining a spectrum. The two-body potential functions used herein to describe the H-Ar, Cl-Ar, and Ar-Ar interactions are of a truncated Lennard-Jones type, necessitating the evaluation of an exponential and a 12th power in the pairwise potential. It is well known that the evaluation of exponentials is time consuming relative to "normal" arithmetic and logical operations, and so we have chosen to calculate forces via a table look-up procedure with a fifth-order polynomial interpolation. This procedure is the one suggested by Andrea *et al.*,<sup>22</sup> in their study of the importance of long-range forces on the structure of liquid water. Implementation of this method has led to a 40% decrease in the computer run time per trajectory.

### III. PHONON EFFECTS ON $(\nu, J) \rightarrow (\nu', J')$ LINE SHAPES

We begin by computing line shapes for several vibration-rotation transitions at a fixed surface temperature, 50

K, and comparing these results with ones obtained previously in the static-surface limit. Each spectral line reported here (except for the ones deriving from the transitions involving the highest rotational energies) required the inclusion of 50 to 60 trajectories in order for convergence to be reached, with each trajectory representing a time span of 24.573 ps. (This time interval corresponds to 245 730 integration steps. Values of the dipole moment components are stored every 30 steps, i.e., every 0.003 ps, so that 8192 points are included in the fast Fourier transforms. The theoretical resolution of these calculations is  $1.3576 \text{ cm}^{-1}$ .) In Fig. 1, one will find the result obtained for the line shape pertaining to the  $0 \leftrightarrow 1$  rotational transitions of the fundamental vibrational band ( $\nu = 0 \rightarrow \nu' = 1, v_c = 1/2$ ). (As we noted in I, choosing an initial action variable to be the arithmetic mean of the quantum numbers indexing the initial and final states leads to  $J_c = 1/2$  being the appropriate classical action variable for describing both  $J = 0 \rightarrow J' = 1$  and  $J = 1 \rightarrow J' = 0$ .) We see that only a single line (a Q branch) arises from the calculations and not the two [ $R(0)$  and  $P(1)$ ] that would be expected if this were gas-phase HCl. Such a result is consistent with the rotational dephasing line broadening mechanism noted in I, characterized by an averaging to zero of the molecular angular momentum vector. More to the point here, though, is a comparison of this line shape with the one found using the static-surface model of I; Fig. 2 gives both results plotted on the same axes. Clearly the inclusion of surface motion (phonon modes) has led to a shift of intensity out of the peak center and into the wing structure, but this shift is not accompanied by a loss of total intensity (for the moving-surface calculation, the integrated peak intensity is found to be  $5.0 \times 10^{-3} \text{ D}^2$ , while in the static-surface case, the negligibly different value  $4.9 \times 10^{-3} \text{ D}^2$  is obtained). The change in the line shape is actually more significant than one might guess just from looking at the linewidth (FWHM), since the data in Table I indicate that only a  $2 \text{ cm}^{-1}$  broadening is associated with "turning on" the surface motion. In this system, we relate the line shape change to an enhanced rate of dephasing and a greater perturbation of the adsorbate motion. Perhaps the most useful way of thinking about the effect of surface motion here is not that it leads to appreciable energy transfer between the adspecies and the surface, but rather that it produces an effective roughening of the surface

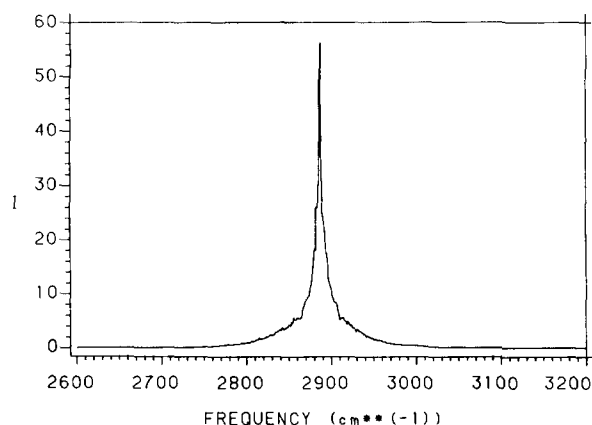


FIG. 1. Spectrum of adsorbed  $^1\text{H}^{35}\text{Cl}$ ,  $\nu = 0 \rightarrow 1$  and  $J = 0 \leftrightarrow 1$ , at 50 K.

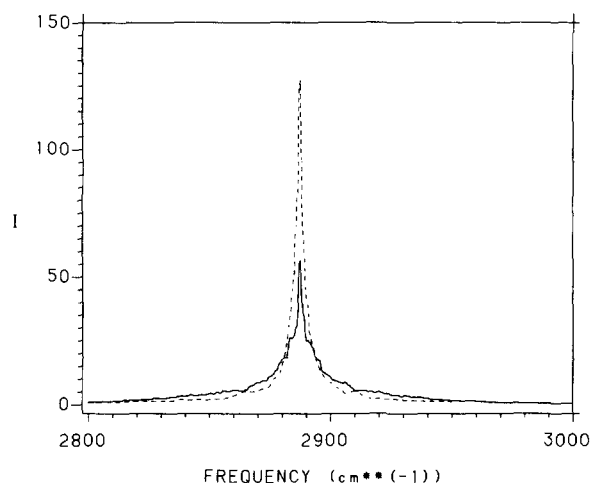


FIG. 2. Spectra of  $^1\text{H}^{35}\text{Cl}$ ,  $\nu = 0 \rightarrow 1$  and  $J = 0 \leftrightarrow 1$ , at 50 K determined from a moving-surface model (solid line) and a static-surface model (broken line).

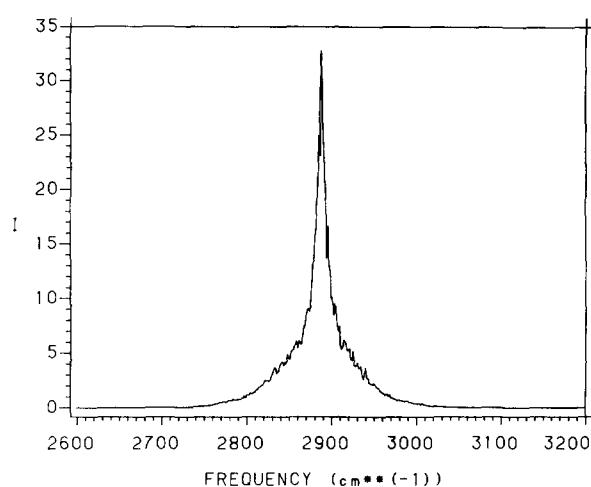


FIG. 3. Same as in Fig. 1, but for  $J = 1 \leftrightarrow 2$ .

which increases the probability of any collision, elastic or inelastic, between the rotating molecule (consisting primarily of H-atom motion) and an Ar atom.

If the rotational energy of the HCl molecule is increased such that the trajectories model the  $J = 1 \leftrightarrow 2$  transitions, the line broadening increases and even more intensity is homogeneously shifted outward away from the peak center (see Fig. 3 and Table I). Again the intensity at the peak center is only about half the value that one would calculate using a static-surface model even though the total integrated intensity is not changed. We also interpret this broadening in terms of an increase in the frequency of dephasing collisions. But of more interest are the  $J = 2 \leftrightarrow 3$  transitions, with the calculated line shape being given in Fig. 4. Note first that there appears to be but a negligible difference between this intensity function and the one corresponding to  $J = 1 \leftrightarrow 2$  that appears in Fig. 3. Although from the data listed in Table I one would conclude that the addition of rotational energy has produced an appreciable broadening of the line, a more detailed comparison reveals the differences to be only slight; any variation in the linewidths is attributable to small changes in the central peak heights and to a lack of smoothness in the peak contours that stems from the inclusion of a fairly small number of trajectories (on the order of 60). Thus, the addition of surface motion in the  $J = 1 \leftrightarrow 2$  case

leads to an increase in the dephasing rate that is comparable with the effect produced when more rotational energy is fed into the adsorbate initially. Actually, the rate in the  $J = 2 \leftrightarrow 3$  case is now so fast that not even the surface motion influences it; the result that we obtained in I for this line shape in the static-surface limit is indistinguishable from what one finds in Fig. 4! It would, therefore, seem true on the basis of these observations that significant phonon effects are going to show up only in the lowest-energy rotational transitions, although these transitions are, of course, the most significant ones at the low temperatures described in the present work.

However, as we have shown previously, there is another dynamical regime in the HCl/Ar(111) system, one that is entered when the adsorbed molecule is excited to high rotational states. Consider, for example, the  $J = 10 \leftrightarrow 11$  transition, for which we have calculated discrete  $R(10)$  and  $P(11)$  lines in our earlier static-surface study. Figure 5 shows that with the inclusion of surface motion, again two adsorption ranges are observed, but no longer do we find a pair of sharp peaks. We hesitate to draw too many conclusions on the basis of these results since only a few trajectories are includ-

TABLE I.  $^1\text{H}^{35}\text{Cl}/\text{Ar}(111)$  spectral lines at 50 K:  $\nu = 0 \rightarrow 1$ .

$J \leftrightarrow J'$ transition	Number of trajectories	Peak position ( $\text{cm}^{-1}$ )	FWHM ( $\text{cm}^{-1}$ )
$0 \leftrightarrow 1$	59(60) <sup>a</sup>	[129(130)] <sup>b</sup> 2887 [2887]	6 [4]
$1 \leftrightarrow 2$	63(70)	[80(80)] 2887 [2887]	8 [6.5]
$2 \leftrightarrow 3$	55(60)	[79(81)] 2887 [2887]	12.5 [7]
$10 \leftrightarrow 11$	27(120)	[62(81)] 3070 [3080] 2660 [2640]	20 [5.5] 25 [11]

<sup>a</sup> The number in parentheses represents the total number of trajectories generated; it differs from the preceding number by the number of desorptive trajectories.

<sup>b</sup> The results in square brackets are those previously calculated using a static-surface model.

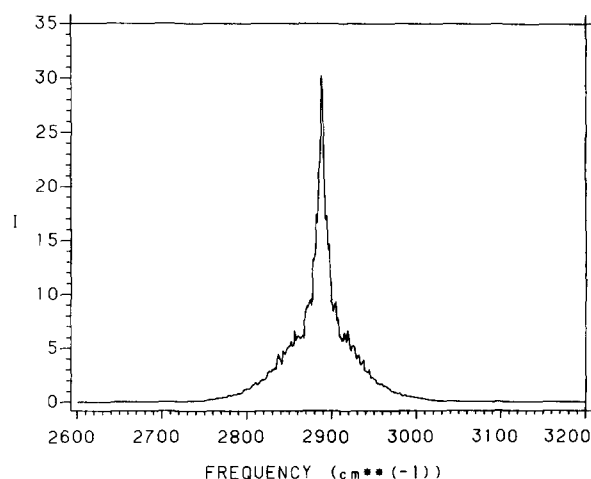
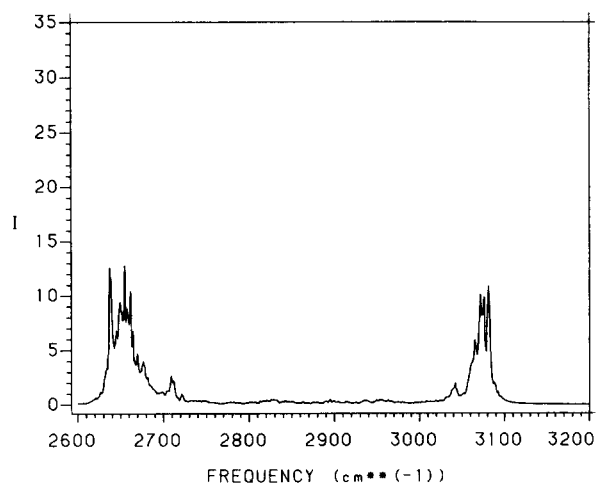


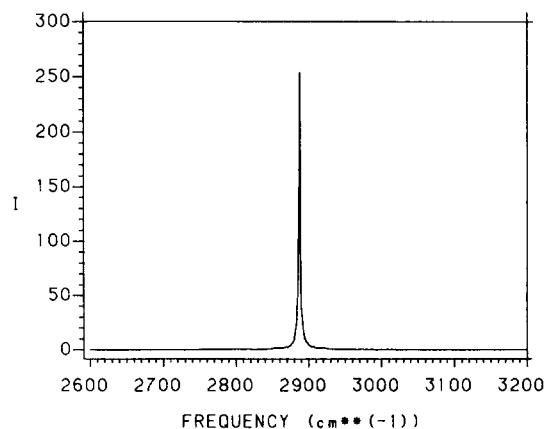
FIG. 4. Same as in Fig. 1, but for  $J = 2 \leftrightarrow 3$ .

FIG. 5. Same as in Fig. 1, but for  $J = 10 \leftrightarrow 11$ .

ed (the desorption rate for molecules with high rotational energies is greatly enhanced in the moving surface model—here there is a 78% probability of desorption within the 24.573 ps trajectory time in contrast to the 23% probability found when the surface atoms were held fixed), but it does seem clear that the broad absorption bands are characteristic of this dynamical regime. It is possible, however, to pick out peaks from the bands that are located exactly at the positions of the sharp features found in the static-surface spectra. To explain these observations we recall that the static-surface results are consistent with a dynamical model in which the molecule may be viewed essentially as a free rotor, with the rotation occurring on the average in a plane parallel to the surface. At these rotational energies, the rotation is sufficiently rapid that the molecule-surface interaction is effectively averaged over a unit cell, and so only the zeroth Fourier component of the potential contributes significantly to the overall interaction. “Turning the surface on,” however, makes the net interaction between the surface and the rapidly rotating molecule more complex since the symmetry of the surface now has been broken. Higher-order Fourier components of the potential therefore enter the picture and as a result the perturbation of the rotating molecule is greater.

#### IV. EFFECT TO TEMPERATURE ON THE $J=0 \leftrightarrow 1$ TRANSITIONS

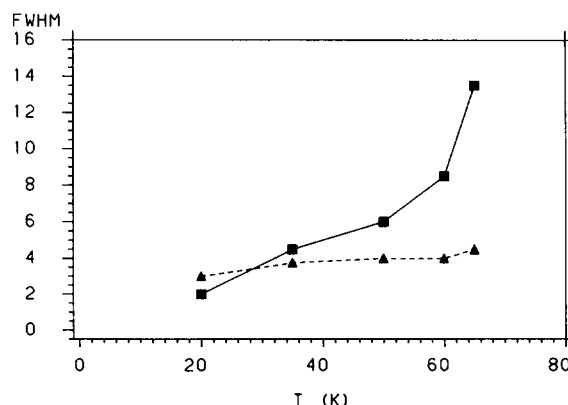
We now focus our attention on what surely are two of the most important spectral transitions in the low temperature HCl/Ar(111) system, these being the  $(0,0) \rightarrow (1,1)$  and  $(0,1) \rightarrow (1,0)$  transitions. (The temperatures over which the system is stable are not high enough to allow for significant population of more than the first few rotational states; in order for one to observe the transitions between the higher rotational states, it first will be necessary to prepare the initial states involved in those transitions via careful irradiation at the appropriate frequencies.) These calculations have been carried out in the same manner as those reported in Sec. III except for the choice of equilibrium system temperature. Changing that temperature, of course, necessitates the regeneration of the initial configuration snapshots, since the particular Monte Carlo random walk algorithm used in

FIG. 6. Spectrum of adsorbed  $^1\text{H}^{35}\text{Cl}$ ,  $v = 0 \rightarrow 1$  and  $J = 0 \leftrightarrow 1$ , at 20 K.

the determination of these configurations yields atomic positions consistent with a specific selected temperature.

We begin with the lowest-temperature system, that being one which has been equilibrated at 20 K, and calculate the line shape function displayed in Fig. 6. At this temperature, the peak is very sharp and narrow, with the FWHM being roughly  $2 \text{ cm}^{-1}$ , which is just slightly greater than the approximately  $1.4 \text{ cm}^{-1}$  theoretical resolution of these calculations. A comparison with the line shape of Fig. 1 calculated for a system temperature of 50 K clearly indicates a decrease in the frequency of dephasing collisions at the lower temperature, even though the initial rotational energies are the same in the two cases. What is missing, of course, at  $T = 20 \text{ K}$  is the enhancement of the dephasing rate coming from a significant thermal distortion of the surface. This result can be seen more clearly in Fig. 7, where we give the temperature dependence of the linewidth determined both for the moving-surface model and for the static-surface model. Note that at the lowest temperature there is no appreciable difference between the two values of the FWHM (we do not assign any significance to the fact that the moving-surface model apparently yields a slightly narrower line than does the static-surface model—the two FWHM values are probably the same within the errors in the calculations).

Increasing the equilibrium temperature to 35 K (see Fig. 8 and note in particular the change in the scaling on the

FIG. 7. Temperature dependence of the  $^1\text{H}^{35}\text{Cl}$   $v = 0 \rightarrow 1$  and  $J = 0 \leftrightarrow 1$  linewidths for the moving-surface (squares) and the static-surface (triangles) models.

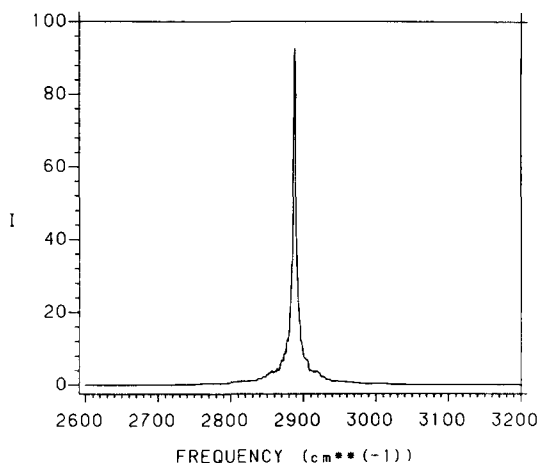


FIG. 8. Same as in Fig. 6, but for  $T = 35$  K.

vertical axis) clearly broadens the calculated spectral line and begins the shift of intensity away from the peak center and into the wings. However, the situation is still not too different from what we see when the surface atoms are held fixed. It is not until we reach about 50 K (again refer to Fig. 7) that a clear divergence is seen between the two dynamical cases, with this difference becoming even more pronounced as the temperature is increased further. The line shape obtained for the highest temperature studied here, 65 K (above this temperature it becomes increasingly likely that sublimation events will occur which destroy the integrity of the surface slab over the lifetime of the trajectory), is broadened considerably and is more like those found at higher rotational energies (Fig. 9) but lower surface temperatures. Again, a good way of viewing this effect is in terms of an effective roughening of the surface as the temperature is increased and the thermal displacements of the surface atoms become larger.

While it is not possible to compare directly our results with experimental ones due to an absence of such measurements on the HCl/Ar(111) system, we do wish to call attention to work by Trenary *et al.*<sup>23</sup> concerning the spectrum of CO chemisorbed at various sites on a Ni(111) surface. Although there obviously are very great differences between

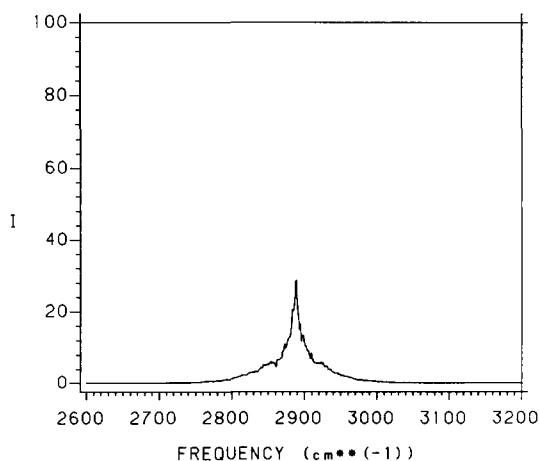


FIG. 9. Same as in Fig. 6, but for  $T = 65$  K.

this system and ours, there is one interesting similarity, that being the suggested interpretation of the linewidths obtained for each in terms of a dephasing mechanism. In particular we note that for these two systems one finds the temperature dependence of the linewidths to be qualitatively of the same form, with a marked increase in the widths being observed at the high end of the temperature range.

Finally, we should mention that there actually is a second sort of temperature dependence that might be envisioned for the spectrum of a physisorbed molecule, that being one related to the increase in the rate of lateral diffusion with temperature. One would suspect that as diffusion increases, there will be an increasing likelihood of collisions occurring that lead to dephasing irrespective of whether or not surface phonon modes are active. As we see from the static-surface results plotted in Fig. 7, though, such an effect appears to contribute very little to the overall temperature dependence. We thus conclude that for practical purposes in our system, all the temperature dependence is attributable to motion of the surface atoms. (In an experimental system one of course would also be seeing effects arising as a consequence of the temperature dependence of the relative populations of initial states.)

## ACKNOWLEDGMENTS

The calculations in this paper have been performed on a IBM 3090 mainframe computer, access to which has been made possible through a grant from the IBM Corporation. The author wishes to thank the staff of the Palo Alto Scientific Center, and in particular W. C. Swope, for their suggestions concerning this work and for their assistance in using their facilities.

<sup>1</sup>See, for example, *Vibrations at Surfaces*, edited by R. Caudano, J. M. Gilles, and A. A. Lucas (Plenum, New York, 1982); *Vibrational Spectroscopies for Adsorbed Species*, ACS Symp. Ser. No. 137, edited by A. T. Bell and M. L. Hair (American Chemical Society, Washington, D.C., 1980).

<sup>2</sup>Ph. Avouris, D. Schmeisser, and J. E. Demuth, *Phys. Rev. Lett.* **48**, 199 (1982).

<sup>3</sup>S. Andersson and J. Harris, *Phys. Rev. Lett.* **48**, 545 (1982).

<sup>4</sup>R. E. Palmer and R. F. Willis, *Surf. Sci.* **179**, L1 (1987).

<sup>5</sup>J. E. Adams, *J. Chem. Phys.* **84**, 3589 (1986).

<sup>6</sup>(a) D. W. Noid, M. L. Koszykowski, and R. A. Marcus, *J. Chem. Phys.* **67**, 404 (1977); M. L. Koszykowski, D. W. Noid, and R. A. Marcus, *J. Phys. Chem.* **86**, 2113 (1982); (b) D. M. Wardlaw, D. W. Noid, and R. A. Marcus, *ibid.* **88**, 536 (1984).

<sup>7</sup>K. S. Sorbie, *Mol. Phys.* **32**, 1577 (1976); K. S. Sorbie and N. C. Handy, *ibid.* **32**, 1327 (1976); **33**, 1319 (1977); N. DeLeon and E. J. Heller, *J. Chem. Phys.* **78**, 4005 (1983); W. H. Miller, *ibid.* **81**, 3573 (1984).

<sup>8</sup>See, for example, D. Langreth, *Phys. Rev. Lett.* **54**, 126 (1985); A. Liebsch, *ibid.* **54**, 67 (1985).

<sup>9</sup>J. R. Stein and D. W. Noid, *J. Chem. Phys.* **78**, 1876 (1983).

<sup>10</sup>P. H. Berens and K. R. Wilson, *J. Chem. Phys.* **74**, 4872 (1981).

<sup>11</sup>For a good overview of methods for determining vibrational lineshapes of adsorbed molecules, including trajectory methods, see J. W. Gadzuk and A. C. Luntz, *Surf. Sci.* **144**, 429 (1984); J. W. Gadzuk, *J. Electron Spectrosc. Relat. Phenom.* **38**, 233 (1986).

<sup>12</sup>R. G. Gordon, *Adv. Magn. Reson.* **3**, 1 (1968).

<sup>13</sup>A. Papoulis, *Probability, Random Variables, and Stochastic Processes* (McGraw-Hill, New York, 1965), pp. 336–352.

<sup>14</sup>P. F. Naccache, *J. Phys. B* **5**, 1308 (1972).

<sup>15</sup>T. A. Weber and F. H. Stillinger, *J. Chem. Phys.* **80**, 2742 (1984).

<sup>16</sup>D. J. Diestler, *J. Chem. Phys.* **78**, 2240 (1983).

- <sup>17</sup>J. F. Ogilvie, W. R. Rodwell, and R. H. Tipping, *J. Chem. Phys.* **73**, 5221 (1980).
- <sup>18</sup>See, for example, J. D. Doll and H. K. McDowell, *J. Chem. Phys.* **77**, 479 (1982); J. E. Adams and J. D. Doll, *ibid.* **80**, 1681 (1984).
- <sup>19</sup>J. P. Valleau and S. G. Whittington, in *Statistical Mechanics; Part A*, edited by B. J. Berne (Plenum, New York, 1977).
- <sup>20</sup>See, for example, R. N. Porter and L. M. Raff, in *Dynamics of Molecular Collisions; Part B*, edited by W. H. Miller (Plenum, New York, 1976).
- <sup>21</sup>W. C. Swope, H. C. Andersen, P. H. Berens, and K. R. Wilson, *J. Chem. Phys.* **76**, 637 (1982).
- <sup>22</sup>T. A. Andrea, W. C. Swope, and H. C. Andersen, *J. Chem. Phys.* **79**, 4576 (1983).
- <sup>23</sup>M. Trenary, K. J. Uram, F. Bozso, and J. T. Yates, Jr., *Surf. Sci.* **146**, 269 (1984).